

On the Nitrogen Diffusion in a Duplex Stainless Steel

Margarita Bobadilla^{a*}, Andre Tschiptschin^a

^aMetallurgical and Materials Engineering Department, University of São Paulo – USP,
Av. Prof. Mello Moraes, 2463, CEP 05508-900, São Paulo, SP, Brazil

Received: October 12, 2014; Revised: February 16, 2015

Duplex Stainless Steels (DSS) have excellent corrosion resistance properties and poor wear resistance. Plasma nitriding is used to increase the surface hardness, by nitrogen diffusion into the crystal lattice, and to improve wear resistance. In this study, DSS samples were plasma nitrided at temperatures between 350 °C and 500 °C for 240 minutes under an atmosphere of 75% N₂ + 25% H₂. Apparent diffusion coefficients, activation energy and pre-exponential constant were calculated using the first law of Fick for each material phase, austenite and ferrite. Nitrogen diffusion in both phases appears to be similar. The layer thickness on the alpha phase is greater than in the gamma phase. Nevertheless, the difference on the layer thickness in both of the phases is small. From these results, it was proposed a model of nitrogen diffusion into a two-phase stainless steel to explain the morphology of the interface between the layer and the substrate.

Keywords: plasma nitriding, duplex stainless steel, nitrogen diffusion, expanded austenite

1. Introduction

Duplex stainless steels (DSS) are used in applications where they must have good wear resistance properties, having a good resistance to corrosion. To accomplish this, DSS are submitted to thermochemical treatments as plasma nitriding to increase the surface hardness^{1,2}, wear resistance³ and fatigue properties⁴. Nitriding is done at low temperatures to prevent nitrides formation, which reduces corrosion resistance⁵. Hardening is given by the nitrogen diffusion into the crystal lattice. Although the mechanism of diffusion of nitrogen in austenitic stainless steels (ASS) has been extensively studied⁶⁻⁸. In the case of DSS there are studies where nitrided layer properties are evaluated^{5,9,10}, but the mechanism of formation and the morphology of the layer have not been deeply studied^{11,12}. This study aims to study the kinetics of nitrided layer formation on DSS and its morphology.

2. Material and Methods

The material used in this study was a duplex stainless steel with 0.01% C 3.06 Mo 5.82% Ni 21.89% Cr Fe in balance chemical composition. Specimens of 20×10×5 mm were cut, plasma nitrided and characterized by Scanning Electron Microscopy (SEM). Before nitriding, perpendicular to lamination direction face of the specimens was mechanically ground and polished with diamond paste down to 1 μm.

Passive film was removed through a sputtering step of pure Argonium plasma at 350 °C for 1 hour. Specimens were DC-plasma nitrided on the perpendicular to lamination direction face at 350, 400, 450 and 500 °C for 240 minutes in a 75% N₂ + 25% H₂.

Nitrided layers, obtain for each temperature, were measured on the micrographs using a conversion of the rule present on the photographs and the real distance on them.

3. Results and Discussion

Microstructures of nitride layers, for each temperature, are present on Figures 1 to 4.

Table 1 shows that temperature increase leads to formation of thicker nitrided layers.

Diffusion coefficients were calculated as function of layer thickness obtained for each treatment temperature, using the Equation 1

$$d=(Dt)^{(1/2)} \quad (1)$$

where “d” is the thickness layer, “D” is the diffusion coefficient for nitrogen and “t” is the treatment time. In addition, shown on Table 2.

Calculated diffusion coefficients for austenite and for ferrite are apparent for nitrogen diffusion in each phase. In theory, coefficients of ferrite phase should have around two orders of greatness rather than coefficients for nitrogen in austenitic phase. This is because the nitrogen diffusion in this system is not completely explained by Fick’s first law (solid state diffusion)¹³. There are other associated mechanisms, which will be explained later.

It was not possible to find any study in literature that report diffusion coefficients values, for nitrogen in a duplex stainless steels for nitriding at low temperature. By comparing the values of the coefficients of Table 2 and those reported in literature for austenitic stainless steel, it can be seen that the diffusion coefficients found in this study to austenite even with different microstructure are similar to those found in the literature^{8,13-15}, they are of the same order of magnitude.

*e-mail: maroboga@gmail.com

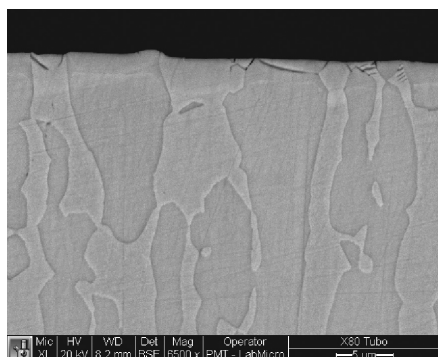


Figure 1. Nitrided layer obtain at 350 °C.

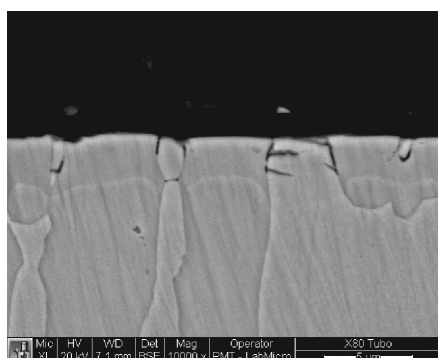


Figure 2. Nitrided layer obtain at 400 °C.

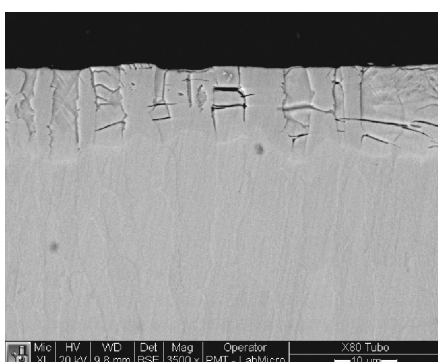


Figure 3. Nitrided layer obtain at 450 °C.

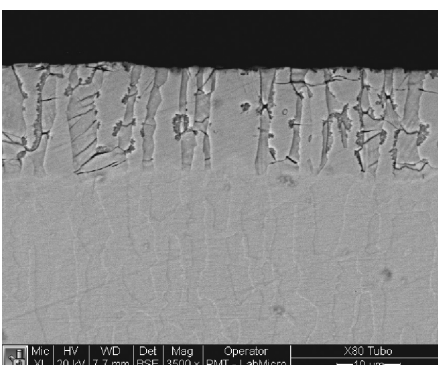


Figure 4. Nitrided layer obtain at 500 °C.

Table 1. Layer thickness obtained for each plasma nitriding treatment for austenite and ferrite phases.

Temperature °C	Experimental Thickness (µm)	
	Austenite	Ferrite
350	2.0	2.4
400	2.3	3.3
450	11.6	13.4
500	19.6	20.6

Table 2. Calculated diffusion coefficients for each phase and nitriding temperature from the experimental layer thickness

Temperature °C	D (m ² /s)	
	Austenite	Ferrite
350	2.73386E-16	4.06908E-16
400	3.769E-16	7.45612E-16
450	9.32314E-15	1.24172E-14
500	2.6668E-14	2.9348E-14

Furthermore, when comparing the values of the coefficients found for austenitic stainless steels is noticed that are not equal, even though it has the same crystal structure. These results show that nitrogen diffusion into the crystalline lattice of stainless steel depends on microstructure of the material, alloying elements present^{8,16}, and crystallographic orientation (texture)^{13,17}. In the specific case of single crystal (111)¹⁷, the estimated coefficient is very close to that found in this work for the austenitic phase.

From the curve $\ln D$ vs. $1/T$ in Figure 5, it is possible to determinate the activation energy and pre-exponential constant.

Some authors calculated the diffusion coefficients from mathematical models that describe the diffusion process of nitrogen in austenitic stainless steel. Moskaliuviene¹³ calculated that the value of the pre-exponential constant was $8.37 \text{ E-6 m}^2 / \text{s}$ and Parascandola¹⁸ assumed for their calculations of nitrogen diffusion profiles a pre-exponential constant of $\text{E-7 m}^2 / \text{s}$. For the activation energy, both Parascandola¹⁸ and Möller¹⁹ assumed to his calculations the value of 1.1 eV. Comparing the activation energy values reported on literature with those calculated for the austenitic phase of the duplex stainless steel in this study, the difference was only 0.18 eV. This suggests that diffusion in the austenitic phase of duplex stainless steel has an energy barrier similar to that found for the diffusion of nitrogen in expanded austenite in austenitic stainless steels. It was also observed that ferrite and austenite have similar activation energies. In the case of pre-exponential constant, by comparing the calculated by Parascandola¹⁸ with the calculated in this work, the difference is about an order of magnitude. However, when comparing with the results found by Moskaliuviene¹³, the value is very similar to the pre-exponential constant found in this study. This result was expected because the presence of ferrite in the material in some way influences nitrogen diffusion into austenite phase. This is because an interstitial atom can diffuse faster in a body centered cubic structure (ferrite) than in face-centered cubic structure (austenite), as will be discussed later.

4. Morphology of the Nitrided Layer

Under ideal conditions, assuming that nitrogen diffusion into the equilibrium phases (ferrite and austenite) of iron and that the layer formation was entirely controlled by diffusion volume, it is possible to calculate the layer thickness, knowing the diffusion coefficient at each temperature using Equation 1, sendo $D=D_0\exp(-Q/(RT))$

Where D_0 and Q are the diffusion constants for nitrogen into iron.

In Table 3 are the diffusion coefficients calculated for each theoretical stage, using the theoretical values for nitrogen diffusion, D_0 as 0.0047 cm²/s for ferrite and 0.0034 cm²/s for austenite and Q as 18300 cal/mol for ferrite and 34600 cal/mol for austenite²⁰. Moreover, are listed the theoretical layer thickness. Theoretical layer morphology is presented in Figure 6.

These results, however, consider only unidirectional diffusion in each phase (austenite and ferrite) of duplex stainless steel. According to the theoretical values of thickness of the layer (d) shown in Table 2, whereas unidirectional diffusion, formation of the nitride layer in the material during the nitriding process can be schematized as shown in Figure 6.

This morphology is explained because there is difference of diffusion of nitrogen in the two phases of the material. The diffusion of an atom there are two properties that directly affect, solubility and diffusivity. The solubility is associated with a number of atoms which can stay within the unit cell in this case CFC (austenite) structure can accommodate many more nitrogen atoms therein than CCC structure (ferrite). The diffusivity is associated with the facility that an atom has to move within the crystalline lattice, overcoming barriers formed by substitutional atoms in the lattice. The interstitial atoms can move faster within the body-centered cubic structure because the atom packing factor is lower. Therefore, lower atomic density, which is why it is easier to cross it. Already nitrogen diffusion in austenitic structure is much more difficult due to the higher atom packing factor of CFC structure, compared with the ferritic structure CCC. In summary, the diffusivity is greater in CCC than in CFC structure and solubility is greater in CFC than in CCC. This can explain the thickness difference between the phases.

The theoretical morphology as calculated above, shown in Figure 6 does not correspond to the morphology observed in this study, which is shown schematically in Figure 7.

This morphology was also reported by other authors. Bielawski¹¹ explains that this layer shape demonstrates that diffusion in ferrite and austenite are different. As growth in the ferrite phase is faster than in austenitic phase giving rise to the concavity of the arc formed in the layer. The

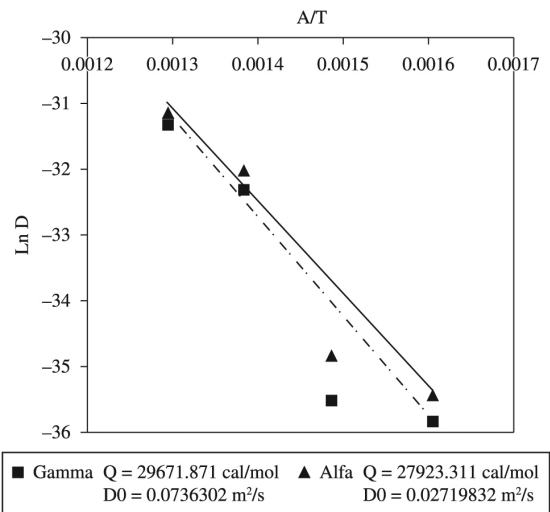


Figure 5. Determination of the activation energy and de preexponential constant using a linear regression.

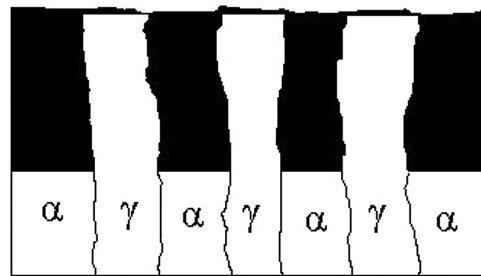


Figure 6. Theoretical morphology of the nitrided layer. Only is considered bulk nitrogen diffusion.

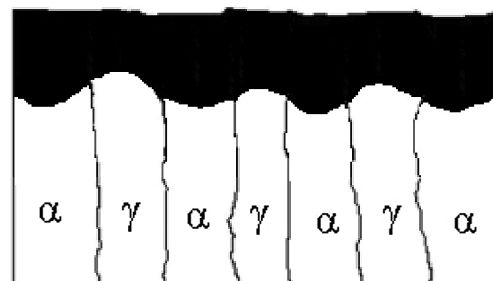


Figure 7. Experimental morphology of the nitrided layer.

Table 3. Theoretical values of diffusion coefficients and layer thickness for each phase and temperature

Temperature °C	Theoric diffusion coef (cm ² /s)		Theoretical layer thickness (um)	
	Austenite	Ferrite	Austenite	Ferrite
350	2.4701E-15	1.78601E-09	0.059640093	50.7134669
400	1.9704E-14	5.35635E-09	0.168445048	87.82449058
450	1.17939E-13	1.38E-08	0.41210728	140.9683075
500	5.60056E-13	3.14573E-08	0.898042436	212.8344084

layer thickness is greater on the ferritic grain and becomes smaller above the austenitic grain. Christiansen²¹ explains the difference in thickness grain by grain is due to the effect of the difference in the chemical composition of the austenite and ferrite in solubility and diffusivity of nitrogen in the development of expanded austenite.

By comparing the values of the thicknesses theoretical and experimental, presented in Table 1 and 3, for the ferrite phase, theoretical thickness is much greater than that found experimentally. In the austenitic phase, the experimental thickness is much greater than the theoretical. We conclude that the layer formed in the ferrite decreases and that formed in the austenite increases.

Analyzing this result might be thought that the formation of the layer, the phenomenon of diffusion of nitrogen is not just unidirectional, as assumed by the theoretical model (Figure 6).

Actually, there are four nitrogen fluxes that produce the experimental layer morphology:

1. Flux from the atmosphere into the interior of the material: existing nitrogen plasma atoms enters inside the material to form the nitrided layer. This is the main flux of nitrogen and which explains the growth layer inside the material.
2. Grain boundary diffusion: the nitrogen diffusion occurs not only in the volume of the substrate, but also by the grain boundary. This flux explains that this atom to enter the existing phases between gamma and alpha limits, which makes the resulting interface is formed by recesses (Figure 7) and not by a straight line (Figure 6).

References

1. Menthe E, Bulak A, Olfé J, Zimmermann A and Rie K. Improvement of the mechanical properties of austenitic stainless steel after plasma nitriding. *Surface and Coatings Technology*. 2000; 133-134:259-263. [http://dx.doi.org/10.1016/S0257-8972\(00\)00930-0](http://dx.doi.org/10.1016/S0257-8972(00)00930-0).
2. Rao KRM, Mukherjee S, Raole P and Manna I. Characterization of surface microstructure and properties of low-energy high-dose plasma immersion ion-implanted 304L austenitic stainless steel. *Surface and Coatings Technology*. 2005; 200(7):2049-2057. <http://dx.doi.org/10.1016/j.surfcoat.2004.06.035>.
3. Baranowska J, Franklin S and Pelletier C. Tribological behaviour and mechanical properties of low temperature gas nitrided austenitic steel in relation to layer morphology. *Wear*. 2005; 259(1-6):432-438. <http://dx.doi.org/10.1016/j.wear.2005.02.002>.
4. Stinville JC, Villechaise P, Templier C, Riviere JP and Drouet M. Plasma nitriding of 316L austenitic stainless steel: Experimental investigation of fatigue life and surface evolution. *Surface and Coatings Technology*. 2010; 204(12-13):1947-1951. <http://dx.doi.org/10.1016/j.surfcoat.2009.09.052>.
5. Kliuga M and Pohl M. Effect of plasma nitriding on wear and pitting corrosion resistance of X2 CrNiMoN 22 5 3 duplex stainless steel. *Surface and Coatings Technology*. 1998; 98(1-3):1205-1210. [http://dx.doi.org/10.1016/S0257-8972\(97\)00240-5](http://dx.doi.org/10.1016/S0257-8972(97)00240-5).
6. Parascandola S, Möller W and Williamson DL. The nitrogen transport in austenitic stainless steel at moderate temperatures. *Applied Physics Letters*. 2000; 76(16):2194-2196. <http://dx.doi.org/10.1063/1.126294>.
7. Pranevicius, L., Templier, C., Pranevicius, L. L., Meheust, P. & Abrasonis, G. On the mechanism of ion nitriding of an austenitic stainless steel. *Surface and Coatings Technology*. 2001; 135:250-257.
8. Christiansen TL and Somers MAJ. Determination of the concentration dependent diffusion coefficient of nitrogen in expanded austenite. *Int. J. os. Materials Research*. 2008; 99:999-1005.
9. Larisch B, Brusky U and Spies H. Plasma nitriding of stainless steels at low temperatures. *Surface and Coatings Technology*. 1999; 1116-119:205-211. [http://dx.doi.org/10.1016/S0257-8972\(99\)00084-5](http://dx.doi.org/10.1016/S0257-8972(99)00084-5).
10. Pinedo CE, Varela LB and Tschiptschin AP. Low-temperature plasma nitriding of AISI F51 duplex stainless steel. *Surface and Coatings Technology*. 2013; 232:839-843. <http://dx.doi.org/10.1016/j.surfcoat.2013.06.109>.
11. Bielawski J, Baranowska J and Szczecinski K. Microstructure and properties of layers on chromium steel. *Surface and Coatings Technology*. 2006; 200(22-23):6572-6577. <http://dx.doi.org/10.1016/j.surfcoat.2005.11.037>.
12. Souza SD, Kapp M, Olzon-Dionysio M and Campos M. Influence of gas nitriding pressure on the surface properties of ASTM F138 stainless steel. *Surface and Coatings Technology*. 2010; 204(18-19):2976-2980. <http://dx.doi.org/10.1016/j.surfcoat.2010.03.005>.
13. Moskaliuviene T, Galdikas A, Rivière JP, Pichon L. Modeling of nitrogen penetration in polycrystalline AISI 316L austenitic stainless steel during plasma nitriding. *Surface and Coatings*

- Technology*. 2011; 205(10):3301-3306. <http://dx.doi.org/10.1016/j.surfcoat.2010.11.060>.
14. Martinavičius A, Abrasonis G, Scheinost AC, Danoix R, Danoix F, Stinville JC, et al. Nitrogen interstitial diffusion induced decomposition in AISI 304L austenitic stainless steel. *Acta Materialia*. 2012; 60(10):4065-4076. <http://dx.doi.org/10.1016/j.actamat.2012.04.014>.
 15. Galdikas A and Moskališviene T. Modeling of stress induced nitrogen diffusion in nitrided stainless steel. *Surface and Coatings Technology*. 2011; 205(12):3742-3746. <http://dx.doi.org/10.1016/j.surfcoat.2011.01.040>.
 16. Christiansen T, Dahl KV and Somers MJ. Nitrogen diffusion and nitrogen depth profiles in expanded austenite: experimental assessment, numerical simulation and role of stress. *Materials Science and Technology*. 2008; 24(2):159-167. <http://dx.doi.org/10.1179/026708307X232901>.
 17. Martinavičius A, Abrasonis G, Möller W, Templier C, Rivière JP, Declémy A, et al. Anisotropic ion-enhanced diffusion during ion nitriding of single crystalline austenitic stainless steel. *Journal of Applied Physics*. 2009; 105(9):093502. <http://dx.doi.org/10.1063/1.3120912>.
 18. Parascandola S, Möller W and Williamson DL. The nitrogen transport in austenitic stainless steel at moderate temperatures. *Applied Physics Letters*. 2000; 76(16):2194-2196. <http://dx.doi.org/10.1063/1.126294>.
 19. Möller W, Richter E, Parascandola S, Telbizova T and Günzel R. Surface processes and diffusion mechanisms of ion nitriding of stainless steel and aluminium. *Surface and Coatings Technology*. 2001; 136(1-3):73-79. [http://dx.doi.org/10.1016/S0257-8972\(00\)01015-X](http://dx.doi.org/10.1016/S0257-8972(00)01015-X).
 20. Callister WD. *Materials Science and engineering: an introduction*. 832 (Wiley, 2006).
 21. Christiansen T and Somers MJ. Low temperature gaseous nitriding and carburising of stainless steel. *Surface Engineering*. 2005; 21(5-6):445-455. <http://dx.doi.org/10.1179/174329405X68597>.